# CHAPTER 3

# EXPERIMENTAL PROCEDURES

## 3.1 Sample Preparation

All powders and ceramics were produced using various preparation methods as described here.

### 3.1.1 Powder Preparation

There are two conditions for general composition:

- Powders in PZN-PZT system were prepared according to the formula: $x\text{Pb}(\text{Zn}_{1/3}\text{Nb}_{2/3})\text{O}_3\text{-}(1\text{-}x)\text{Pb}(\text{Zr}_{1/2}\text{Ti}_{1/2})\text{O}_3$ , where $x$= 0.1-0.5 to study effect of PZN content.
- Powders in PZN-PZT system were prepared according to the formula: $0.2\text{Pb}(\text{Zn}_{1/3}\text{Nb}_{2/3})\text{O}_3\text{-}0.8\text{Pb}(\text{Zr}_x\text{Ti}_{1\text{-}x})\text{O}_3$ , where $x$= 0.40, 0.45, 0.50, 0.52, 0.55 and 0.60 to study effect of Zr/Ti ratio.

The chemical purity and suppliers are listed in Table 3.1. Regent grade oxides of lead oxide, PbO (Fluka Chemical, 99.9% purity), zirconium dioxide, $ZrO_2$ (RdH laborchemikalin, 99.9% purity), zinc oxide, ZnO (Fluka Chemical, 99.9% purity), niobium pentaoxide, $Nb_2O_5$ (Aldrich, 99.9% purity), and titanium dioxide, $TiO_2$ (RdH laborchemikalin, 99.9% purity), were used as starting materials. PZN–PZT powders were synthesized by the solid-state reaction of these raw materials. Ground mixtures of the powders were required with stoichiometric ratios for the general composition. A McCrone vibro-milling technique was employed in order to combine mixing

capacity with a significant time saving. The milling operation was carried out in isopropanal. High purity corundum cylindrical media were used as the milling media. After vibro-milling for 30 minutes and drying at 120$^{o}$C, the reaction of the uncalcined powders taking place during heat treatment was investigated by themogravimetric and differential thermal analysis (TG-DTA, Shimadzu) in air from room temperature up to 1350$^{o}$C. Based on the TG-DTA results, the mixture was calcined at temperatures between 750 to 950$^{o}$C for 2 hours in alumina crucible to examine the phase formation behavior of PZN-PZT powders. A heating/cooling rate of 20$^{o}$C/min was selected for all of the compositions in this system because it was shown to be effective in reducing the total amount of pyrochlore phase. Diagram of experimental procedure of powder preparation is illustrated in Fig. 3.1

**Table 3.1** Specifications of the component oxide powders used in this study.

| Materials | Purity (%) | Formula weight | Manufacturer |
|---|---|---|---|
| Lead(II)oxide PbO | >99.9 | 223.189 | Fluka Chemical GmbH, Switzerland |
| Zirconium dioxide $ZrO_2$ | >99.9 | 123.223 | RdH laborchemikalin GmbH&Co.KG,France |
| Titanium dioxide $TiO_2$ | >99.9 | 79.898 | RdH laborchemikalin GmbH&Co.KG,France |
| Zinc(II)oxide ZnO | >99.9 | 81.389 | Fluka Chemical GmbH, Switzerland |
| Niobium pentaoxide $Nb_2O_5$ | >99.9 | 265.807 | Aldrich Chemical Company Inc., USA |
| Iron(III)oxide $Fe_2O_3$ | >99.0 | 159.68 | Fluka Chemical GmbH, Switzerland |
| Manganese (IV)oxide $MnO_2$ | >99.9 | 86.94 | Signa-Aldrich Chemical Company Inc., USA |

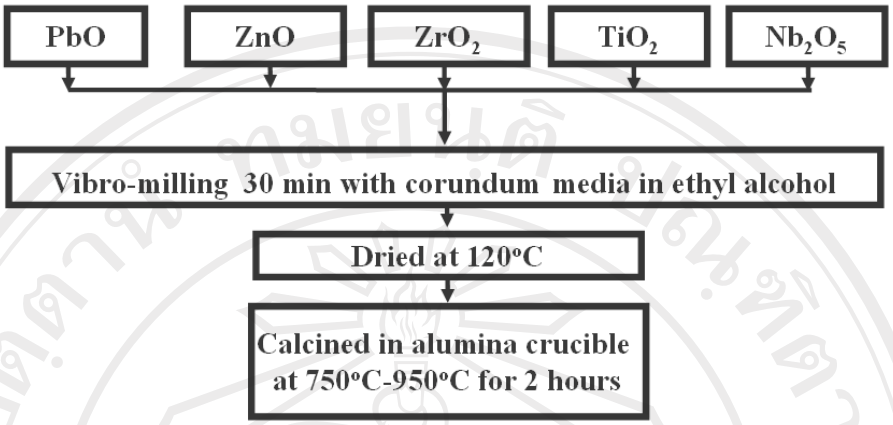


**Figure 3.1** Diagram of experimental procedure on powder preparation.

### 3.1.2 Ceramic Preparation

After calcination, the calcined powders were consolidated into disks of 12.5 mm diameter using isostatic pressing about 150 MPa. Diagram of experimental procedure of ceramic preparation is illustrated in Fig. 3.2.

For *x*PZN-(1-*x*)PZT based-compositions, sintering conditions were selected with temperatures of 1175°C, 1200°C, 1225°C, 1250°C, and 1275°C, and a dwell time of 2 hours.

For 0.2PZN-0.8PZT based-compositions, which were used to study on effect of Zr/Ti ratio and effects of $MnO_2$ and $Fe_2O_3$ addition on electrical properties of PZN-PZT ceramics, sintering condition was selected as 1200°C with a dwell time of 2 hours.

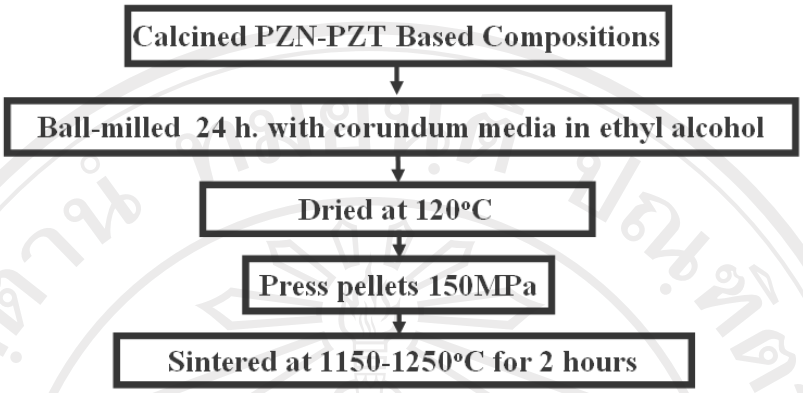


**Figure 3.2** Diagram of experimental procedure on ceramic preparation.

## 3.2 Sample Characterization

All powders and ceramics were characterized using different tools as described below in Fig. 3.3.

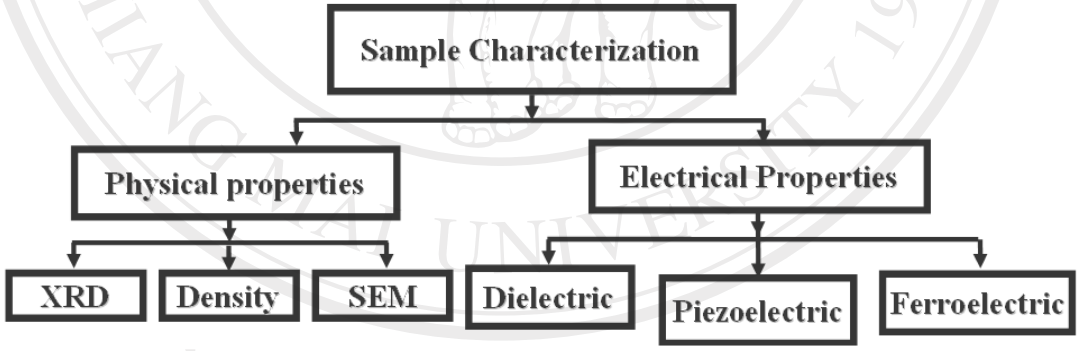


**Figure 3.3** Diagram of experimental procedure on sample characterization.

### 3.2.1 Physical properties

- ***Differential Thermal Analysis (DTA) and Thermogravimetric Analysis (TGA)***

Thermal decomposition and weight loss behaviour of the uncalcined powders was analyzed by Differential Thermal Analysis (DTA) and thermogravimetric analysis (TGA). In this experiment, Perkin Elmer module DTA7 (Fig. 3.4) and Perkin Elmer TGA7 (Fig. 3.5) were employed with platinum crucibles, reference powder of

$Al_2O_3$ and a heating rate of 10 $^oC$/min. The decomposition temperature and weight loss were recorded when the samples were heated from room temperature to 1300 $^oC$.

**Figure 3.4** Differential thermal analysis (Perkin Elmer DTA7)

**Figure 3.5** Thermogravimetric analysis (Perkin Elmer TGA7)

- ***X-ray Diffraction (XRD)***

Calcined and sintered samples were examined by x-ray diffraction (XRD) to insure phase purity. Room temperature XRD patterns were recorded with a Scintag diffractometer using Cu $K_\alpha$ radiation ($\lambda$ = 1.5405 Å) as shown in Fig. 3.6. The pattern were recorded between $2\theta = 10^o$ and $80^o$ at scan rate of $2^o$/ min. A computer

program (MDI Jade v.7.1) was used to determine lattice parameters of the samples upon the X-ray powder diffraction database of ICDD version 2004.

The relative amount of perovskite and pyrochlore phases were estimated from the major peak intensities of the perovskite and pyrochlore peaks using equation [60],

$$\%\,perovskite = \frac{I_{Perovskite}}{I_{Perovskite} + I_{Pyrochlore}} \times 100 \qquad (3.1)$$

where "$I$" represents the intensity of respective phases.


**Figure 3.6** X-ray diffractometer

- ***Scanning Electron Microscopy (SEM)***

In this work, A JEOL JSM-840A and Camscan Series II (Cambridge, England), as shown in Fig. 3.7, were used to determine the morphology of the powders, the as-fired and fracture surface of the ceramics. The powders were dispersed in an ethanol using ultrasonic cleaner, and then coated with gold sputtering. As-sintered surface and fracture surface of the ceramics were cleaned by ultrasonic

cleaner and coated with carbon. During image acquisition, both backscattered and secondary electron modes were used with an accelerating voltage of 20 kV. Chemical composition of the selected area was quantified by using an energy dispersive X-ray spectrometry (EDX). The range of grain size and average grain size were determined by using the linear intercept method [71], where random lines were drawn on a micrograph and the number of grain boundaries intercepting these lines counted. Grain shape of sintering ceramics was classified by using the concept of degree of angularity under ASTM Designation: E112-88 [72].

**Figure 3.7** Scanning electron microscope.

- ***Densification Measurement***

The densities of all samples were determined using the Archimedes' method. The sample is first weighed dry ($W_1$), then weighed again after fluid impregnation ($W_2$), and finally weighed while being immersed in fluid ($W_3$). Generally, a very thin brass wire is used to suspend the sample in the fluid. The density ($\rho$) can be calculated from the following equation:

$$\rho = \frac{\rho' W_1}{W_3 - W_2} \tag{3.2}$$

where $\rho'$ is the density of xylene (0.861g/cm$^3$) at room temperature.

### 3.2.2 Electrical properties

For electrical properties characterizations, silver electrode (Dupont, QS 171) was printed on the lapped surfaces. The electrode was fired at 850$^o$C for 45 min.

- ***Dielectric Measurement***

The dielectric properties of the sintered ceramics were studied as functions of both temperature and frequency with an automated dielectric measurement system in Fig. 3.8. The computer-controlled dielectric measurement system consists of a precision LCR-meter (Hewlett Packard, model 4284A), a temperature chamber, and a computer system. Temperature dependent measurements were performed using a FLUKE 8840 multimeter in conjunction with a temperature chamber. The capacitance and the dielectric loss tangent are determined over the temperature range of 50 and 450 °C with the frequency ranging from 0.1 to 100 kHz.

The dielectric constant was calculated by equation,

$$\varepsilon_r = \frac{Ct}{\varepsilon_0 A} \tag{3.3}$$

where $\varepsilon_r$ and $\varepsilon_o$ are the dielectric constant and permittivity of free space. *C* is the capacitance, and *t* and *A* are the thickness and area of the sample.

**Figure 3.8** Dielectric Measurements system.

- ***Piezoelectric measurement***

The optimum poling conditions were determined by poling the ceramics with applying DC field of 30kV/cm in a stirred oil bath at 150$^{O}$C for a time period 30 minutes as shown in Fig. 3.9. The piezoelectric constant ($d_{33}$) was measured using a quasi-static piezoelectric $d_{33}$ meter (Model ZJ-3d, Institute of Acoustics Academic Sinica, China) in Fig. 3.10. The piezoelectric constant ($d_{33}$) measurements were made directly after poling and after 24 hours. Measurements were conducted at a drive frequency of 100 Hz.


**Figure 3.9** Poling system**.**

**Figure 3.10** Quasi-static piezoelectric $d_{33}$ meter.

The electromechanical properties were also determined under low-power conditions using standard impedance analyzer method. Impedance spectra under low-level constant voltage drive were taken using HP4294A, as shown in Fig. 3.11. From the resonance (impedance maximum) and the anti-resonance (impedance minimum) frequencies, the electromechanical coupling coefficient ($k$), and the mechanical quality factor ($Q_m$) were determined according to IEEE standard methodologies (IRE 1958) [73].

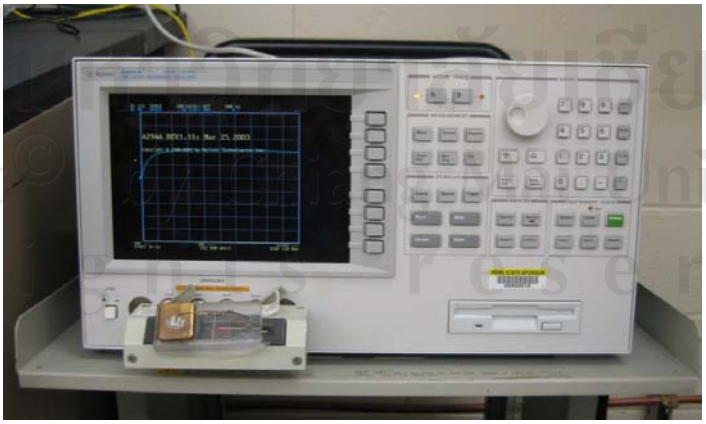

**Figure 3.11** Impedance analyzer HP4294A.

Radial vibration mode in thin disk shape, the planar electromechanical coupling coefficient ($k_p$) can be calculated from equation,

$$k_p^2 = 2.51\left(\frac{f_a - f_r}{f_r}\right) \tag{3.4}$$

The mechanical quality factor ($Q_m$) was determined from the minimum impedance at resonance frequency, $Z_r$ , static capacitance ($C_o$) as equation,

$$Q_m = \frac{f_a^2}{2\pi f_r Z_r C_0 (f_a^2 - f_r^2)} \tag{3.5}$$

where $f_r$ and $f_a$ are resonance and anti-resonance frequency.

- ***Ferroelectric and strain measurements***

Ferroelectric switching measurements, as shown in Fig. 3.12, were made using a modified Sawyer-Tower circuit with a linear variable differential transducer (LVDT) for strain measurement, DSP lock-in amplifier (SR830, Stanford Research), high voltage power supply (TREK 609C-6, Trek), and computerized control and data acquisition. In Fig. 3.13, the system is an automated device intended primarily for measuring the polarization of materials induced by an electric field. It can additionally monitor an external input from LVDT and can compensate for linear displacement in the sample. The frequency range is 1 mHz to 1 KHz and the charge range is ~10pC to100μC.


**Figure 3.12** Ferroelectric and strain measurements.

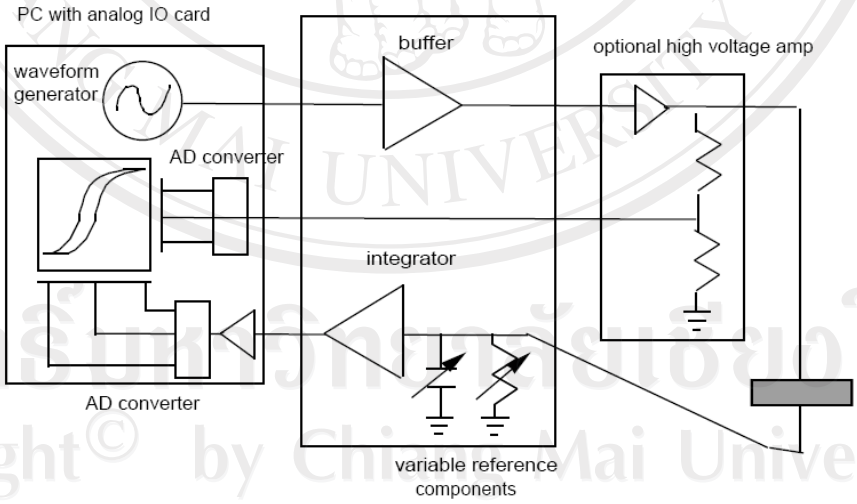


**Figure 3.13** Conceptual block diagram